# On the Extension of LTE and LTE-A PRACH Receiver Design to 5G New Radio

Francesco Linsalata, Maurizio Magarini
DEIB, Politecnico di Milano
Via Ponzio 34/5, 20133 Milan, Italy

Riccardo Ferrari
Azcom Technology s.r.l.
20089 Rozzano, Italy

***Abstract* - Physical random access channel (PRACH) has a key role as interface between the non-synchronized users' equipment and the orthogonal transmission scheme of uplink radio access in wireless cellular communications. Due to stringent requirements in terms of delay and influence of noise and multipath fading on the signal detection, the design of a robust PRACH receiver is a critical issue but, at the same time, it opens the way to the development of new solutions. Moreover, with the introduction of new type of services in fifth generation (5G) new radio systems, i.e. ultra-reliable low-latency and machine-type communications and with the need for mechanisms that are able to dynamically adapt to the changing environment, the design of the PRACH receiver is a priority. With reference to long-term evolution (LTE) and LTE-advanced (LTE-A), in this paper we provide an improvement of PRACH receiver design that reduces the combined effect of missed detection and correct detection, but with the wrong timing advance estimation, probabilities. To this aim, a new three-step approach is proposed to overcome the issues of conventional PRACH signal detection. The benefits of the proposed solution are demonstrated by means of Monte Carlo simulations.**

***Keywords— PRACH, Zadoff-Chu Sequence, LTE, LTE-A, 5G.***

## I. INTRODUCTION

In fourth generation (4G) and fifth generation (5G) standards for cellular communications the physical random access channel (PRACH) is used for the initial network access and for achieving uplink time synchronization of a user equipment (UE) [1]. The first, and the most important, step in the uplink random access procedure, consists in correctly detecting the PRACH preamble signal. In fact, a successful PRACH reception allows for the subsequent UE transmission to be inserted among the scheduled synchronized transmissions of other UEs, thus managing in a proper way the limited frequency-time resources. Also, this allows an accurate estimate of the timing advance (TA), which defines time taken by the signal to reach the base station from the position of the UE. The continuous adaptation of TA reduces the interference, minimizes the data loss, and maintains mobile quality of service.

Several approaches were proposed in the literature for the design of PRACH receivers of 4G long-term evolution (LTE) and LTE-advanced (LTE-A) systems [2]-[5]. All these works consider as a reference against which evaluate the performance a correct detection limit of at least 99%, as outlined in the 3GPP 36.104 specifications [6]. In contrast to previous works and in agreement with 3GPP 36.104 specifications, in this paper the performance is studied with reference to the combined effect of the following three different probabilities of error:

1. $P_d(E)$, which defines the probability of missed detection of the preamble;
2. $P_{ta}(E)$, which defines the probability of wrong TA estimation given that a preamble has been detected;
3. $P_w(E)$, which defines the probability of detection of a preamble other than the one sent.

The sum of these three-error events gives an upper bound of the total missed detection probability:

$$P_{md}(E) \leq P_w(E) + P_d(E) + P_{ta}(E). \quad (1)$$

The classical approach followed in previous works, i.e. [2]-[5], to deal with PRACH detection problem is to cast it in a test of hypothesis framework, where the value of the threshold is calculated by considering the statistics of the signal and the missed detection and false alarm probabilities. The threshold is then used to compare the samples of the power delay profile (PDP) associated with the received signal to decide the presence or the absence of the preamble. In this paper we consider a more practical approach, where the contribution of each term in the right-hand side of (1) is evaluated separately. Considering each term individually allows us to show the main weaknesses of previous approaches, where the presence of side peaks in the PDP increases $P_w(E)$ and $P_{ta}(E)$. The observation of these effects has motivated us to propose a new procedure to reduce both $P_w(E)$ and $P_{ta}(E)$ from a practical point of view, leading to an improvement of the PRACH receiver performance. The proposed method is based on the processing of the PDP with a three steps approach where the samples are recombined and processed in each step. The proposed three-step PRACH signal detection, which is here considered in a 4G setup, can be easily extended to 5G New Radio (NR), which can be interpreted as multi-carrier version of the previous one in the uplink air interface.

The paper is organized as follows. Section II gives a short overview of the preamble sequence construction. Section III outlines the normal detection algorithm, whose issues in real implementation are shown in Sec. IV. Section V describes the proposed algorithm and the numerical results are reported in Sec. VI. Conclusions are drawn in Sec. VII.

## II. PREAMBLE SEQUENCE

The preamble sequences used in LTE and LTE-A are Zadoff-Chu (ZC) sequences, which meet the required ideal auto-correlation property. In fact, it can be shown that ZC sequences satisfy the Constant Amplitude Zero Autocorrelation (CAZAC) property [7]. The prime ZC sequence is defined as

$$x_u(n) = e^{-\frac{j(\pi \cdot u \cdot n \cdot (n+1))}{N_{ZC}}}, \quad (2)$$

where $0 \leq n \leq N_{zc} - 1$, $u$ is the root sequence number, and $N_{zc}$ is the prime length of ZC sequences. They are characterized by several properties, including the ideal cyclic autocorrelation property, which means that the correlation of a sequence, for a fixed $u$, with a circularly shifted version of itself offset of $N_{CS}$ samples is a delta function [7].


Figure 1. PRACH receiver block diagram.

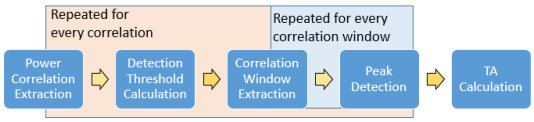


Figure 2. Detection algorithm block diagram

It is worth observing that sequences obtained from cyclic shifts of ZC sequences defined by two different roots are not orthogonal. Hence, orthogonal sequences obtained by cyclically shifting a single root sequence should be favored over non-orthogonal ones. In LTE and LTE-A the preamble sequence is built by cyclic shifts of a ZC sequence of prime length $N_{ZC}$=839. The cyclic shift offset $N_{CS}$ is chosen so that the zero correlation zone (ZCZ) of the sequences, i.e. the number of samples between two peaks, guarantees the orthogonality inside the radius of the cell. In each LTE cell a number of 64 mutually orthogonal sequences is used, all obtained by cyclic shifts the root sequence, see [8], as follows:

$$X_{u,v} = x_u\big((n + C_v) \mathrm{mod} N_{ZC}\big), \tag{3}$$

where mod $N$ denotes modulo $N$ operation and

$$C_V = \begin{cases} vN_{CS} & v = 0,1,\dots,\lfloor N_{ZC}/N_{CS} \rfloor - 1, \quad N_{CS} \neq 0, \\ 0, & N_{Cs} = 0. \end{cases}$$

## III. Conventional PRACH detection

The eNodeB PRACH receiver must be implemented in order to maximize the correct preamble detection probability and minimize the delay due to the processing. The block diagram of the conventional PRACH receiver is illustrated in Fig. 1 [8]. The preamble signal is extracted after cyclic prefix (CP) and guard period (GP) removal, down-sampling, application of fast implementation of discrete Fourier transform (FFT), sub-carrier selection, and correlation in the frequency domain with the local ZC root sequence. The main blocks of Fig. 1 are:

- CP and GP removal;
- frequency shift;
- de-mapping;
- decimation and FFT;
- power delay profile calculation;
- inverse FFT (IFFT)
- detection.

The detection algorithm is implemented in the last block of Fig. 1, whose content is shown in Fig. 2. The classical detection approach starts from the computation of the average power of the correlation, as

$$m_{tot} = \frac{1}{N_{sample}} \cdot \sum_{k=0}^{N_{sample}-1} pdp(k), \tag{4}$$

where $pdp(k)$ is the discrete-time PDP obtained as IFFT of the correlation. The power threshold below which we assume to have only noise is

$$T_{total} = T_{TH} * m_{tot}, \tag{5}$$

where $T_{TH}$ is the optimal threshold computed from the theory, according to a pre-defined probability of false alarm [7]. The threshold $T_{TH}$ can be computed assuming an ideal channel

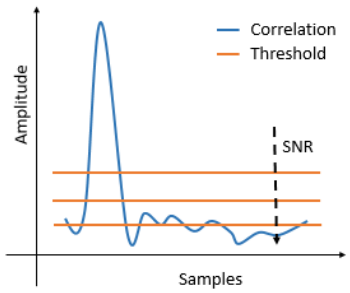


Figure 3. Undesired peaks vs SNR

affected by additive white Gaussian noise (AWGN) as

$$P_{fa} = 1 - (1 - \exp(-N_a \cdot N_{nca} - 1)) \cdot \cdot \sum_{k=0}^{N_a \cdot N_{nca}-1} \frac{1}{k!} \cdot (N_a \cdot N_{nca} \cdot T_{TH})^k, \tag{6}$$

where $N_a$ is the number of antennas and $N_{nca}$ is the number of non-coherent addition, such that $N = N_a \cdot N_{nca}$ is the degree of freedom (DoF).

The above formula holds for a zero-mean complex AWGN, where the power envelope is a central Chi-square distribution whose DoFs are determined by the number of Gaussian random variables that are added together. Extending this concept to complex signals the DoFs are doubled because these signals are the sum of two different random signals. Moreover, since the received signal is defined as the sum of the streams received by each of the two antennas, the resulting DoFs of the received PRACH signal take into account also the number of received antennas. The indexes of the PDP smaller than $T_{total}$

$$\mathcal{K} = \{k_{n_1}, k_{n_2}, \dots, k_{N_{noise}} | pdp(k) < T_{total}\}$$

define the samples that are considered as noise. From these samples, it is possible to calculate the average value of noise as

$$m_N = \frac{1}{N_{noise}} \cdot \sum_{k \in \mathcal{K}} pdp_{noise}(k). \tag{7}$$

Then, the detection threshold used to detect the presence of the preamble is

$$T_{det} = T_{TH} \cdot m_N. \tag{8}$$

Finally, the approach exploits the property of the ZC sequence and implements a window-based detection approach, where the size of the window is the zero-correlation zone of the sequence, i.e. $N_{cs}$ [7]. According to this approach, the presence or absence of a preamble is verified for every window by comparing each sample in the window with the detection threshold level $T_{det}$. The maximum value in the window that is higher than $T_{det}$ is the candidate preamble. Its position inside the window is used to estimate the TA. In this paper, we refer to this approach as one-step PRACH detection algorithm.

## IV. Issues of the One-step PRACH Detection

The one step PRACH detection algorithm is essentially a frequency-domain correlation method. It is worth observing that the higher is the signal-to-noise ratio (SNR), the lower is $m_N$ and, therefore, the detection threshold. In this situation we observed several undesired detections, as exemplified in Fig. 3. These undesired peaks are called side peaks, which are very critical at high SNR values and affect the missed detection

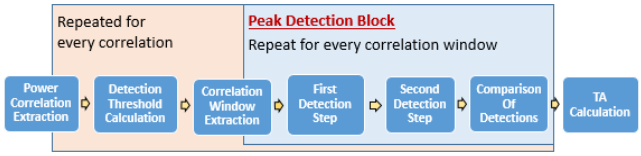


Figure 4. Multi steps detection algorithm

probability by increasing the contribution $P_w(E)$ in (1). This phenomenon happens because the value of the threshold is too low. Hence, a possible solution to deal with this issue, is to increase value of the threshold when

$$\frac{\beta \cdot \max_k pdp(k)}{T_{TH} \cdot m_N} > 1. \qquad (9)$$

The ratio $\max_k pdp(k) / m_N$ can be considered as an estimate of the peak SNR. The parameter $\beta$ in (9), must be set to satisfy the 3GPP conformance requirements [6]. In a high delay spread channel scenario, such as the extended terrestrial urban (ETU) channel defined by International Telecommunication Union (ITU), due to the coherent sum of multipath, which are clarified in the next section, it is empirically computed to distinguish low SNR from high SNR condition. As we will see, the choice of $\beta$ and the correction of the threshold, which leads to a two-step procedure, is not enough to satisfy the 3GPP requirements. The power accumulated on side peaks can exceed the threshold, based on the average noise power, leading to a choice of an incorrect peak and a wrong estimation of the TA. To manage this other issue, we propose to add another step to the detection that leads to the proposed three-step PRACH detection algorithm described in the next section.

## V. Proposed Three-Step Algorith

In this section we illustrate the proposed algorithm, where the threshold in (9) is first modified, as explained in the following, and then the problem of finding the correct position of the peak inside the window is addressed.

The side peaks are a critical issue in high delay spread scenarios. Starting from this observation, for each simulation we keep track of the number of corrections and no-corrections of the threshold value and, also, of the presence of more than one value that is exceeded, in the considered correlation window, the updated or not updated threshold. If this happens there are two possible error cases:

1. an error due to the correction of the threshold;
2. an error due to the non-correction of threshold.

Considering all the simulations, the probability of error due the correction or non-correction of the threshold is also found as

$$P(E) = P(E|correction) \cdot P(correction) + P(E|non-correction) \cdot P(non-correction),$$

where P(correction) is given by the number of simulations for which (9) is verified, divided by the total number of simulations and $P(E|correction)$ the number of times for which is found more than one peak, also after the threshold correction. The other ones are computed consequently. The results for different SNR conditions, considering an ETU channel, are reported in Table 1. As it can be observed, threshold-based SNR adaptation does not always guarantee a null probability of error, because of the presence of the multipath. To solve this issue the proposed approach is based on the idea of combining a predetermined

Table 1. Conditioned probability of error after threshold correction (left) and non-correction (right) for different SNR values

| | Conditioned probability of error | |
|---|---|---|
| **SNR (dB)** | Without threshold correction | With threshold correction |
| **-20** | 0.0001 | 0 |
| **-18** | 0.0011 | 0 |
| **-16** | 0.001 | 0 |
| **-14** | 0.0011 | 0 |
| **-12** | 0.0008 | 0 |
| **-10** | 0.0005 | 0 |
| **-8** | 0.00132 | 0 |
| **-6** | 0.00164 | 0.00118 |
| **-4** | 0.00314 | 0.00112 |
| **-2** | 0.00568 | 0.00138 |
| **0** | 0.01473 | 0.00178 |
| **2** | 0.03648 | 0.00102 |
| **4** | 0.07692 | 0.00136 |
| **6** | 0.23529 | 0.00141 |
| **8** | 0.2 | 0.0011 |

number of adjacent samples in the time to condense the effect of the channel in the actual position of the correlation. This allows us to reduce the side peak power and, at the same time, to increase accuracy of TA estimation. The resulting algorithm is depicted in Fig. 4. The detailed steps are as follow:

*1)* As explained in section IV, what we first find empirically is the value of $\beta$. After many simulations we obtain that a good choice is 0.0315. Then, if (9) is verified in the considered searching window, an updated threshold is calculated, and the number of corrections or non-corrections of the threshold value done in the different simulations, is updated. This is expressed mathematically as

$$if\ (9)\quad then\ T_{det}^{updated} = \beta \cdot \max_k pdp(k). \qquad (10)$$

In the first detection step, the proposed approach processes, one after the others, small and overlapping intervals of the entire PDP. This is done considering the trend of $P_{fa}$ for different uncertain interval length (6). An interval length of 15 samples is obtained from:

$$\frac{N_{IFFT}}{N_U - 1} + 1, \qquad (11)$$

where $N_{IFFT}$ is the size of the IFFT to generate the PDP in time domain and $N_U$ is equal to $\lfloor N_{ZC}/N_{CS} \rfloor - 1$ (see section III). The starting point $k$ of each interval are found empirically:

$$window_k = pdp(i) \quad for\ i = k{:}\,k+1$$

with $k \in \mathcal{K}$ ={0 1008 992 976 961 945 929 913 897 881 865 849 834 818 802 786 770 754 738 723 707 691 675 659 643 627 611 596 580 564 548 532 516 500 485 469 453 437 421 405 405 389 373 358 342 326 310 294 278 262 247 231 215 199 183 167 151 135 120 104 88 72 6 40 24}.

For each $window_k$, if a new threshold is calculated using (10), the position and the value of the peak in the considered

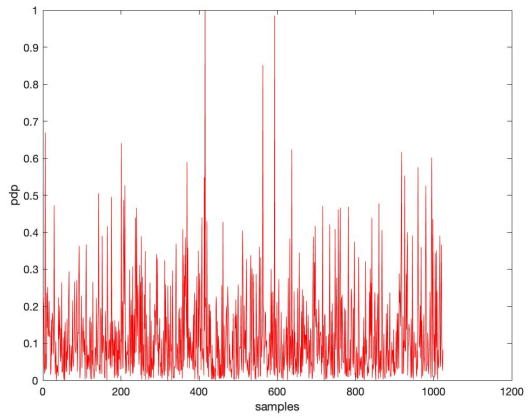


Figure 5. Normalized PDP

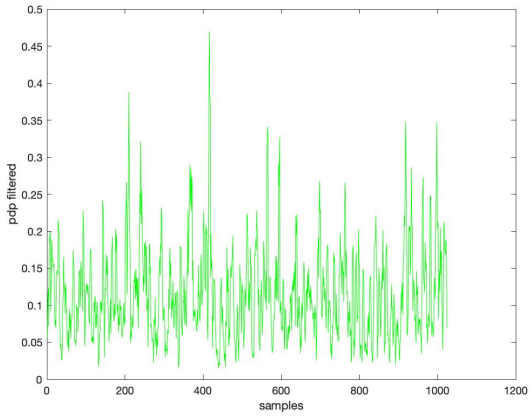


Figure 6. Normalized and filtered PDP

interval is determined as

$$peak - value_k = \max\big(pdp(window_k)\big). \quad (12)$$

*2)* In this step we follow the same approach as that proposed in [9], where a filtering operation is introduced if the peak value is greater than $T_{det}$. The filtering operation is done on the $k$th $window_k$ with the goal of reducing the effect of the delay spread. To this aim, a moving average filter is applied. Since the searching window has dimension much less than $N_{CS}$, the length of the filter could not be too long otherwise the timing advance estimation is affected. The length of this filter, found after several simulations, is

$$L = \left\lceil \frac{N_{IFFT}}{N_{ZC}} \cdot c \right\rceil, \quad (13)$$

where $c$ is a constant value, in our case equal to 5, and $\lceil\ \rceil$ is the lowest integer greater than its argument. In the filtered window the position and the value of its peak is determined and compared with the given threshold.

$$if\ peak - value_k > T_{det} \quad (14)$$

$$then\ filter - window_k = window_k * \mathrm{rect}\left(\frac{k}{L}\right) L$$

$$peak - value'_k = \max\big(pdp(filter - window_k)\big)$$

where $*$ denotes convolution and

$$\mathrm{rect}(k) = \begin{cases} 1, & -\lceil (L-1)/2 \rceil \le k \le \lfloor (L-1)/2 \rfloor \\ 0, & otherwise \end{cases}.$$

As we can see, in Figs. 5 and 6, the effect of the moving average filter on the entire PDP is that of reducing the side peaks due to multipath scenario.

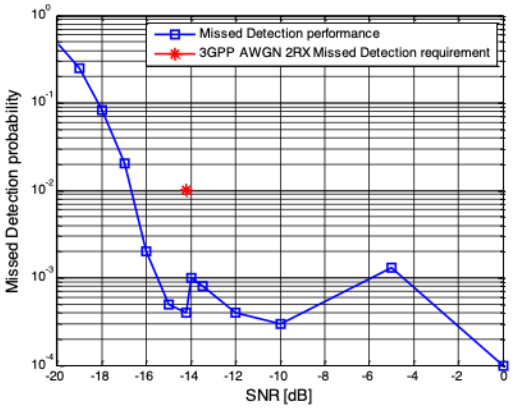


Figure 7. AWGN performance, single step receiver

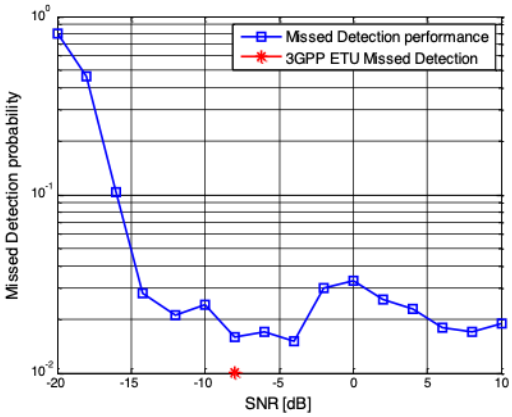


Figure 8. ETU performance, single step receiver

*3)* In the last step it is decided which detection is the most reliable between the two steps, checking if

$$peak - value'_k \cdot L > peak - value_k. \quad (15)$$

The delay offset is calculated and the TA is updated considering the winning peak position and an interpolation approach. The proposed algorithm, in case of correct preamble detection, takes into account: i) the probability of error (1); ii) the reliability of the estimated TA, and how it affects the missed detection probability. This is achieved by calculating $P_{ta}(E)$, which is the number of times for which the algorithm correctly finds the preamble but overestimates the TA, leading to an error. The obtained results are shown in Tab. 2. Note that, the decision if a detection is happened or not is different at low and high SNR scenario. For the low SNR scenario, a detection happens if at least in one of the two steps there is a cross of the threshold. In the high SNR scenario, a detection happens if in both the steps there is a crossing of the threshold. This is done to reduce the error detection due by side peaks.

When a detection happens there are two different situations:

1. only one step has a crossing of the detection: its information is taken as correct;
2. both the steps have a detection: the peak with the higher power is considered as the most reliable one.

Another important result to note is that with the introduction of the second step $P(E|correction)$ and $P(E|non-correction)$ go to zero, with an order of magnitude less than $10^{-4}$ for all the SNR values considered in Table 1.

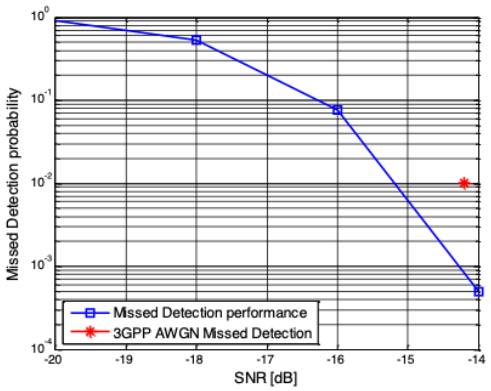


Figure 9. AWGN performance, multi-step receiver

Table 2. Probability of wrong estimated TA for different SNR value

| SNR (dB) | Prob. of error of the |
|---|---|
| **-20** | 0.0011 |
| **-18** | 0.0013 |
| **-16** | 0.0022 |
| **-14** | 0.0026 |
| **-12** | 0.0033 |
| **-10** | 0.0021 |
| **-8** | 0.0030 |
| **-6** | 0.0021 |
| **-4** | 0.0030 |
| **-2** | 0.0019 |
| **0** | 0.0030 |
| **2** | 0.0020 |
| **4** | 0.0022 |
| **6** | 0.0020 |
| **8** | 0.0020 |
| **10** | 0.0021 |

## VI. NUMERICAL RESULTS

In this section the performance of the proposed approach is reported and compared with that of the one step algorithm. The considered scenarios are those defined in [6], the most relevant of which are reported in Table 3. In what follows we do not show any result for the false alarm probability since it is below the value of $10^{-3}$ for both the channel scenarios as defined in TS 36.104. The missed detection probability versus SNR for the single step detector is reported in Figs. 7 and 8 for the AWGN and the ETU70 scenarios, respectively. Numerical results for the proposed multi-step detector are reported in Figs. 9 and 10.

A comparison of the results shows that for the AWGN channel there is not any significant difference between the two detection algorithms. It is worth observing that a wrong selection in the design of the key factors could lead to a worse performance for this scenario, since the AWGN channel is only one tap channel. Threfore, a trade-off between the two different scenarios must be done in the selection of the key parameters. On the other side for the ETU channel, the proposed detection algorithm allows to satisfy the stringent requirements defined in [6]. Results for other bandwidths are not shown because they

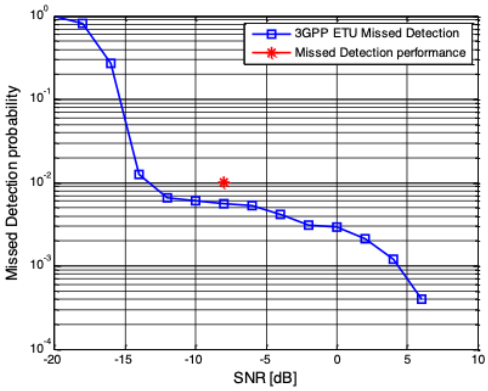


Figure 10. ETU performance, multi-step receiver

Table 3. Parameters used in the simulations

| Parameter | Value |
|---|---|
| **System bandwidth** | 20 MHZ |
| **PRACH Format** | 0 |
| **Channel** | AWGN/ETU70 |
| **Doppler** | 0/200 [HZ] |
| **RX Antenna** | 2 |

are very similar to those we have reported here.

## VII. CONCLUSION

The paper focuses on practical issues arising in the detection of the PRACH signal. A new three-step PRACH detector is proposed that faces with these problems and allows to satisfy the 3GPP requirements. Computer simulations demonstrate the effectiveness of the proposed solution compared to the conventional one step approach. The proposed approach originally designed for 4G cellular systems can be directly extended to 5G NR.

## VIII. REFERENCES


[1] R.-G. Cheng *et al.,* "Two-phase random access procedure for LTE-A networks," IEEE Trans. Wirel. Commun, March 2019.

[2] C. Yu, *et al.*, "Random access algorithm of LTE TDD system based on frequency domain detection", in Proc. ICSKG, pp. 346-350, 2009.

[3] S. Kim, K. Joo, and Y. Lim, "A delay-robust random access preamble detection algorithm for LTE system", IEEE Radio and Wireless Symposium, 2012.

[4] M. Mansour, "Optimized architecture for computing zadoff-chu sequences with application to LTE", in Proc. GLOBECOM, pp. 1-6, 2009

[5] L. Wu, X. Zhang, and Y. Yang, "Design and realization of baseband signal downsampling in LTE System", International Journal of Future Generation Communication and Networking, pp. 81-88, 2013.

[6] 3GPP, "3rd Generation Partnership Project; Technical Specification Group Radio Access Network NR Base Station (BS) radio transmission and reception, 36.104", 2018

[7] S. Sesia, M. Baker, and I. Toufik (2011) LTE-the UMTS long term evolution: from theory to practice. John Wiley & Sons

[8] 3GPP, "Technical Specification Group Radio Access Network; Evolved Universal Terrestrial Radio Access (E-UTRA); Physical channels and modulation, 36.211", 2018

[9] Y. Zhang, Y. Liu, and Z. Zhang, "Simulation and implementation of PRACH signal detection in LTE-A," Journal of Computer Applications, pp. 1-7, Feb. 2018.